Adv. Studies Theor. Phys., Vol. 4, 2010, no. 7, 305 - 316

Dynamics of the Shock Wave Accompanied by Nanoparticle Formation in the PLA Processes

T. Takiya[1], N. Fukuda[1], N. Inoue[1], M. Han[2], M. Yaga[3] and Y. Iwata[4]

[1]Hitachi Zosen Corporation, 2-2-11 Funamachi, Taisho, Osaka 551-0022, Japan
takiya@hitachizosen.co.jp

[2]Department of Materials Science and Engineering, Nanjing University, 22 Hankou Road, Nanjing 210093, China

[3]Faculty of Engineering, University of the Ryukyus, Senbaru- 1, Nishihara, Okinawa 903-0213, Japan

[4]Advanced Institute of Science and Technology, 1-1-1 Umezono, Tsukuba, Ibaraki 305-8568, Japan

Abstract

In the present article, we describe the process of nanoparticle formation during pulsed laser ablation in an inert gas atmosphere. We investigated the interaction between laser ablated plumes and shock waves using one-dimensional Eulerian fluid dynamics equations combined with a rate equation relating to a classical nucleation model of supersaturated vapours. We found a certain case wherein the rate of nanoparticle formation becomes higher when a reflected shock wave passes through the plume. In that particular case, the nucleation and nanoparticle growth can be carried out as separate processes.

Keywords: shock wave, nanoparticle, laser ablation

1 Introduction

Pulsed laser ablation (PLA) has been used as an effective technique to produce nanoparticles with a precisely specified size. Production of nanoparticles with the desired size is made possible because the conditions for evaporated mass and ambient gas pressure can be independently controlled in this technique. The

interaction between the plume and the ambient gas play an important role in nanoparticle formation. Spectroscopic experiments have been conducted by other groups with the aim of investigation into the plume dynamics during the PLA process [1]. However, shock waves were generated in the early stage of the PLA and were resulted to extensive reflection and diffraction of them, which makes the clarification of the nanoparticle formation process increasingly difficult. Hitherto, no attempt to introduce shock wave generation and reflection into the plume dynamics has been reported in relation to nanoparticle formation. Some of the authors have demonstrated that a thermodynamic confinement could occur using the interference between the shock wave and the plume [2], followed by the formation of atomic clusters in the confinement region which are uniform in size and electronic state, and so developed a new laser ablation type cluster source named "spatiotemporal confined cluster source" (SCCS), which gives well-defined thermodynamic conditions of density and temperature in the gas phase [4].

In the present paper, the authors demonstrate the dynamics of the shock wave and the plume relevant to nanoparticle formation by solving the one-dimensional fluid equation. The plume was supposed to be generated immediately after PLA in a closed space regarded as the SCCS. A qualitative prediction of the nanoparticle formation was described from a viewpoint of macroscopic fluid dynamics based on classical nucleation theory.

2 Numerical procedures

For the governing equations, we have chosen the one-dimensional compressible Eluerian equations. The equations were solved by a finite volume method using a type of total variation diminishing (TVD) scheme. The calculations were carried out on 1000 grids. The third-order Runge-Kutta scheme was adopted for time integration in order to simulate the traveling shock wave interacting with the moving plume. The calculations were done based on the FORTRAN code developed by a part of the authors [9].
The basic conservation equations of mass, momentum and energy for the unsteady one-dimensional flow of a vapour and an inert gas in Eulerian coordinates may be expressed as

$$\frac{\partial \mathbf{Q}}{\partial t} + \frac{\partial \mathbf{E}}{\partial x} = \mathbf{W} \tag{1},$$

$$\mathbf{Q} = \left[\rho_v \quad \rho_g \quad \rho_m u \quad e \quad C_1 \quad C_2 \quad C_3 \quad C_4\right]^{\mathrm{T}} \tag{2},$$

$$\mathbf{E} = \left[\rho_v u \quad \rho_g u \quad p + \rho_m u^2 \quad (e+p)u \quad C_1 u \quad C_2 u \quad C_3 u \quad C_4 u\right]^{\mathrm{T}} \tag{3},$$

$$\mathbf{W} = \left[-\dot{\rho}_c \quad 0 \quad 0 \quad \lambda\dot{\rho}_c \quad I \quad \dot{r}C_1 \quad 2\dot{r}C_3 \quad 4\pi\dot{r}C_3 \right]^{\mathrm{T}} \tag{4}.$$

Here, x and t are independent space and time coordinates and ρ, u, p and e express the density, flow velocity, pressure and total energy per unit volume respectively. The values of the vapour, inert gas and their mixture are denoted by the subscripts v, g and m respectively. The factor of λ is the latent heat of vapour or nanoparticle species. Both the dotted variables of $\dot{\rho}_c$ and $\dot{r}$ are temporal differentiations which indicates the increasing rates of cluster density and cluster radius, respectively. The variable I is called nucleation rate, which represents the number of critical clusters generated per the unit volume and time. While the indexed variables, C_1,C_2,C_3 and C_4 are always temporary, the last one , C_4, only denotes the cluster density , ρ_c, itself.

The rate equation for the density of nanoparticles was evaluated by integrating the mass along the particle trajectory,

$$\dot{\rho}_c = 4\pi\rho_l \left\{ I\frac{r_*^3}{3} + \frac{dr}{dt}\int_{t_i}^{t} I\left(r_* + \int_{\tau}^{t}\frac{dr}{dt}d\theta \right)^2 d\tau \right\} \tag{5}.$$

In the rate equation, ρ_l is the bulk density of nanoparticle species. The variable I was used as a nucleation rate of the so-called classical theory [8]. The critical radius and the growth rate of a nanoparticle can be introduced based on the classical nucleation theory as follows:

$$I = \frac{n^2 c v_c}{4r_*}\sqrt{\frac{3W_*}{\pi kT}}\exp\left(-\frac{W_*}{kT}\right) \tag{6},$$

$$r_* = \frac{2\sigma v_c}{kT\ln S} \tag{7},$$

$$\frac{dr}{dt} = \xi v_c \sqrt{\frac{kT}{2\pi m}}\left(n - n_\infty\right) \tag{8}.$$

Here, n is the number density of vapour, c is the thermal velocity of the vapour atom, W_* is the Gibbs free energy of critical cluster formation, k is Boltzman constant, T is temperature, σ is the surface tension, v_c is the volume per atom, S is supersaturation, ξ is the condensation coefficient and m is the mass of the atom. The variable n_∞ means the number density at equilibrium condition.

The initial conditions are given at $t = 0$, based on a stochastically thermodynamic calculation [3] and Knudsen analysis [6]. Laser is irradiated onto a silicon target by the fluence of 25500 $\mathrm{Jm^{-2}}$ and the pulse duration of 1.0 ns. The target surface temperature reached a maximum value of 6100 K during laser pulse irradiation,

and the temperature after Knudsen layer was evaluated at 4080 K using Knudsen analysis. The total number of vapour atoms counted was 1.61×10^{14} within a definite period in which the surface temperature was higher than the boiling point. The vapour density at the early stage just after the laser irradiation was 1.54 kgm^{-3}. A shock tube problem was solved in the calculation space in which both boundaries at x=0 and x=20 mm were solid walls and the initial pressure of helium gas was kept at 100 Pa.

3 Results and discussion

The density profiles of the silicon plume, helium gas and nanoparticle calculated in the area between two solid walls are shown in Fig.1. The density distributions in an early stage of ablation are shown in Fig. 1(a). At the earlier stage, a lot of nanoparticles were formed near the left side wall, and eventually transported downwards by convection as seen from the continuous series of density distributions. Although the vapour plume expanded and pushed the buffer gas away, the expansion did not continue. Since the ejection of the ablated plume from the target surface is limited to a very short time, the plume was pushed back from the buffer gas and was compressed. In the compressed region, the supersaturation becomes very high, resulting in clustering and nanoparticle formation. It was clearly observed that a shock wave was generated in front of the plume and this propagates into the buffer gas. Interestingly, the shock wave transmitted was faster than the plume (Fig.1 (b)). The peak in the plume density gradually decreased with time, while the nanoparticle density increased. In Figs.1 (b) and 1(c), the shock wave is shown colliding with the right side wall. Furthermore, the peak in the nanoparticle density deviated from that of the vapour plume. The reflected shock wave intensified and collided with the plume as shown in Fig.1 (d). Figure 1(e) shows the wave patterns immediately after the collision. The shock wave penetrated into the plume raising its density and the plume was forced back and slightly moved to the left as in Fig.1 (d) and Fig.1 (e). Immediately after the shock wave passed through the plume, the nanoparticle density increased exponentially. Furthermore, a substantial increase in the particle radius was observed and the value of radius reached around 1.5 nm but no nucleation was observed during this period (data not shown). This clearly shows that radius increase and nuclear generation are two independent factors, and that only the radius increase is greatly affected by the reflected shock wave.

The intensity profiles of light emission in the plume, which had been captured by a high speed CCD camera, were plotted along the longitudinal axis as shown in Fig. 2. These series of profiles mean that the plume was expanding in the closed space filled with buffer gas. It could be estimated from other considerations based upon spectroscopic experiments that the most part of emission intensity stems from the relaxation process of silicon dimmer which has been excited by collisions between silicon vapour atoms [4]. The emission of plume might be therefore strongly correlated with the vapour density.

As shown in Fig.2, the plume expansion through the following phases: (a) the early stage of formation of the compressed contact front; (b) rightward shifting of the fully developed contact front; (c) almost arrival at the right side wall of the space; (d) interference with the reflected shock wave bouncing back from the right wall, followed by further rise of the intensity. The condition of plume expansion is nearly consistent with that of vapour density calculated by the present procedure, as stated above. This could give qualitative validity of the calculation procedure.

Let us consider temporal variations about spatially averaged nanoparticle parameters, such as the total mass of clusters, nucleation rate, integrated number of nuclei and cluster size.

Figure 3(a) shows the time variation of total mass of nanoparticles in the enclosed space. The abscissa is the time in logarithmic scale, which is convenient for expressing several different phenomena, which occur with various time scales. After the mass of nanoparticles increased to 0.1 μs, the mass became stable after 0.1 μs and increased again at 10 μs. The time of the second increase in the mass corresponds with the time when the reflected shock wave was transmitted to the plume.

Figure 3(b) indicates the time variation of total nucleation rate evaluated in the space. This is the derivative value, which represents the formation rate of cluster nucleus at any given instance. After the nucleation rate gradually increased until time reached to 0.01 μs, a rather sudden decrease was seen until 0.1 μs.

On the other hand, the total number of nucleus is a temporally integrated value. The time dependency of nucleus number also integrated in the space is shown in Fig.3(c). Since the numbers are saturated at t = 0.01 μs, it is clearly seen that the nucleation has been completed in the early stage of expansion, as expected from Fig.3 (b). Unlike the mass of nanoparticles, the nanoparticle number was not affected by the reflected shock wave.

The averaged cluster size, $\overline{N}_c$, which is denoted by the following equation, will now be discussed,

$$\overline{N}_c = \frac{4\pi\overline{r}^3}{3v_c} \tag{9}.$$

Here, $\overline{r}$ is the averaged cluster radius at a provided position and time as below,

$$\overline{r} = \sqrt{\frac{C_3}{C_1}} \tag{10}.$$

The variables C_1 and C_3, which have been mentioned in equations (2), (3) and (4), are expressed as follows:

$$C_1(t) = \int_{t_i}^{t} I(\tau)d\tau \tag{11},$$

$$C_3(t) = \int_{t_i}^{t} I(\tau)\left(r_*(\tau) + \int_{\tau}^{t} \frac{dr}{dt} d\theta \right)^2 d\tau \quad (12).$$

The variable C_1 represents the total number of cluster nucleus integrated along the particle trajectory, as well as the variable C_3, which is proportional to the total surface area of the nanoparticles.
The further spatially averaged size of nanoparticles in the enclosed space is shown in Fig.3 (d). The value of size reached around 1000, which is consistent with the value obtained by the other experiment, where silicon clusters of 2 to 3 nm in diameter were formed by pulsed laser ablation in an enclosed space filled with a helium buffer gas [5]. Since the nanoparticles are concentrated in the narrow region near the interface between the plume and the buffer gas, the averaged value is considered to be a typical value at the region. The size began to increase at t = 0.001 μs, and continued to gradually increase until t = 0.1 μs. A second increase in size was observed at t = 10 μs when the reflected shock wave passes through. The increase was so large as to actually determine the nanoparticle size. A substantial increase in the size was observed after t =10 μs, which was greatly attributed to the effect of the reflected shock wave, and the size increase was completely separated from the nuclear increase. Such separation may be preferable for generating mono-dispersed nanoparticles.

It could then be estimated that the pressure increase during the reflected shock wave passing is more effective than the temperature increase for acceleration of nanoparticle growth, since the pressure is directly connected with collision frequency needed in the growth. In order to determine this, the increases of pressure and temperature as well as the growth rate caused by the shock wave will be calculated here. For the calculation, Rankine-Hugoniot equations were used as follows[7]:

$$\frac{p_2}{p_1} = \frac{b(\rho_2/\rho_1) - 1}{b - (\rho_2/\rho_1)} \quad (13),$$

$$\frac{T_2}{T_1} = \frac{(p_2/p_1) + b}{b + (p_1/p_2)} \quad (14).$$

Here, subscripts 1 and 2 denote the states in front of the shock wave and behind it, respectively. And the constant b is expressed as follows:

$$b = \frac{\gamma + 1}{\gamma - 1} \quad (15).$$

Here, γ is the ratio of specific heat.
The state variables behind the shock wave were calculated with use of Eqs. (13) and (14). A certain state in the plume actually simulated above was selected as the state ahead of the shock wave. Just before the reflected shock wave passed through, the leading edge of the plume possessed a state wherein the pressure was 325 Pa and the temperature was 982 K.

Calculated pressure and temperature after the shock wave passed away are expressed as ordinate in Fig. 4(a), while Mach number ahead of shock wave was set as abscissa. In addition, rates of condensation and evaporation, and the net growth rate of nanoparticle are plotted in Fig. 4(b). The net rate is derived by subtracting the evaporation rate from the condensation rate.
It is clearly seen from Fig. 4(a) that the pressure increase is more sensitive than the temperature increase against the rise of the Mach number. On the other hand, it can also be seen that condensation is influenced by pressure, just as evaporation is strongly affected by temperature. Condensation rate increases linearly with vapour pressure increase, since condensation results from collisions between nanoparticles and vapour atoms. Compared with this, the evaporation rate rapidly increases after the temperature exceeds the melting point, followed by an exponential rise. The evaporation rate is maintained at such a small value below the melting point that condensation is shown to be the dominant phenomena. There could be a possibility to enhance nanoparticle growth by using the shock wave if the temperature does not exceed the melting point.

4 Conclusions

In the present calculations, the formation of nanoparticles during pulsed laser ablation was analyzed numerically by solving the fluid dynamic equations with nucleation terms. Based on the results, we may conclude that the possibility exists to form nanoparticles using pulsed laser ablation in an enclosed space filled with a buffer gas. In the numerical results and also in the experiment on light emission in the plume, we found that the calculated profiles of vapour density are correlated with the intensity profiles of light emission captured by a high-speed camera. Since the emission of plume might be strongly correlated with the actual vapour density from the other consideration based on the experiment, this fact could give qualitative validity of the calculation procedure. On the other hand, the existence of certain conditions for nanoparticle formation in the narrow region between the plume and the buffer gas were confirmed from the numerical results. In addition, reflected shock waves substantially contribute to the growth of nanoparticles by increasing particle radius, but do not contribute to the increase of nanoparticle numbers by promoting nucleation.

References

[1] D. B. Geohegan, A. A. Puretzky, G. Duscher and S. J. Pennycook, Time-resolved imaging of gas phase nanoparticle synthesis by laser ablation, Appl. Phys. Lett., 72-23(1998), 2987-2989.

[2] M. Han, Y. Gong, J. Zhou, C. Yin, F. Song, M. Muto, T. Takiya and Y. Iwata, Plume dynamics during film and nanoparticles deposition by pulsed laser ablation, Phys. Lett., A302 (2002), 182-189.

[3] F. A. Houle and W. D. Hinsberg, Stochastic simulation of heat flow with application to laser–solid interactions, Appl. Phys., A66 (1998), 143-151.

[4] Y. Iwata, M. Kishida, M. Muto, S. Yu, T. Sawada, A. Fukuda, T. Takiya, A. Komura and K. Nakajima, Narrow size-distributed silicon cluster beam generated using a spatiotemporal confined cluster source, Chem. Phys. Lett., 358(2002), 36-42.

[5] Y. Iwata, M. Muto, T. Sawada, M. Han, A. Fukuda, S. Okayama, H. Matsuhata, H. Yamauchi, M. Kishida, T. Takiya, A. Komura and K. Nakajima, Well-defined Cluster Beam Deposition (CBD) Developed for Vacuum Synthesis of Nanostructures, Proc. 5th ISTC Scientific Advisory Committee Seminar, Nanotechnologies in the area of physics, chemistry and biotechnology, St. Petersburg, Russia, 27-29 May, 2002.

[6] C. J. Knight, Theoretical Modeling of Rapid Surface Vaporization with Back Pressure, AIAA J., 17-5(1979), 519-523.

[7] A. H. Shapiro, The Dynamics and Thermodynamics of COMPRESSIBLE FLUID FLOW, Ronald Press, New York, 1953.

[8] P. P. Wegener, Nonequilibrium Flow with Condensation, Acta Mech., 21(1975), 65-91.

[9] M. Yaga, T. Takiya and Y. Iwata, Numerical study of unsteady compressible flow driven by supersonic jet injected into elliptical cell with small exit hole, Shock waves, 14-5/6(2005), 403-411.

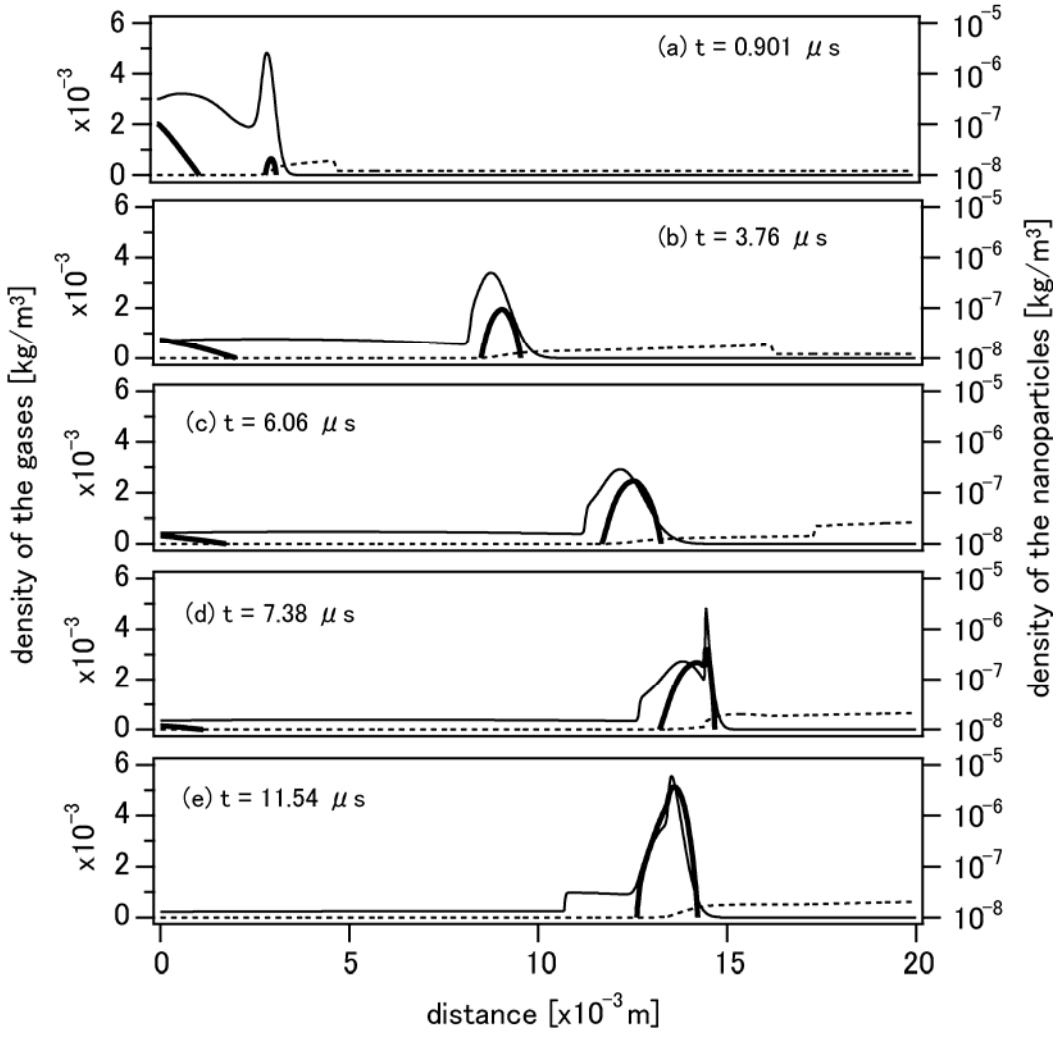

Fig.1 A time sequence of the density distribution of the laser ablated silicon plume (thin solid line), the helium buffer gas (dotted line) and the nanoparticle (thick solid line).

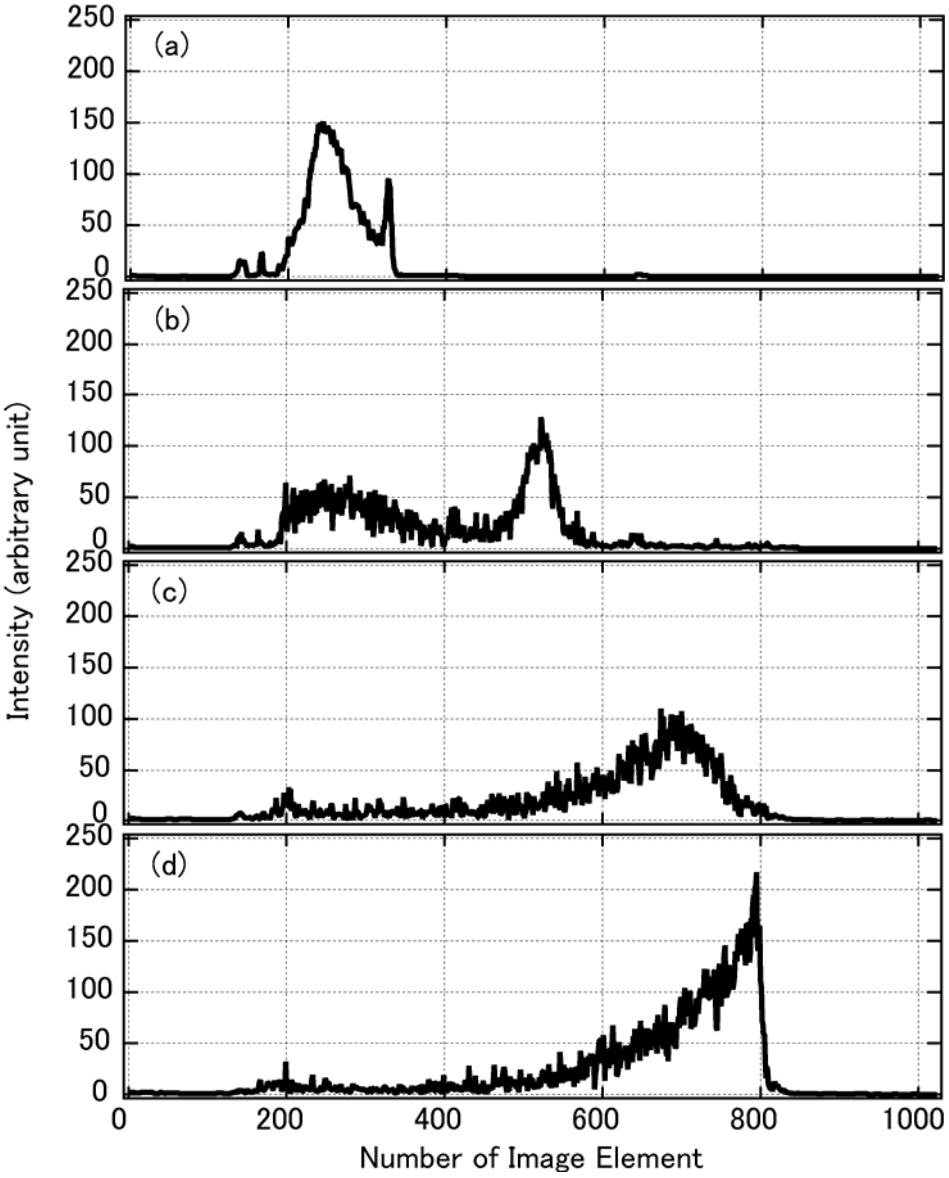

Fig.2 Intensity profiles derived from a series of light emission images of plume captured by a high speed camera; (a) the early stage of formation of the compressed contact front, (b) rightward shifting of the fully developed contact front (sensitivity of the camera was quadruplicated from here), (c) almost arrival at the right side wall of the space, (d) interference with the reflected shock wave bouncing back from the right wall, followed by a further rise of the intensity.

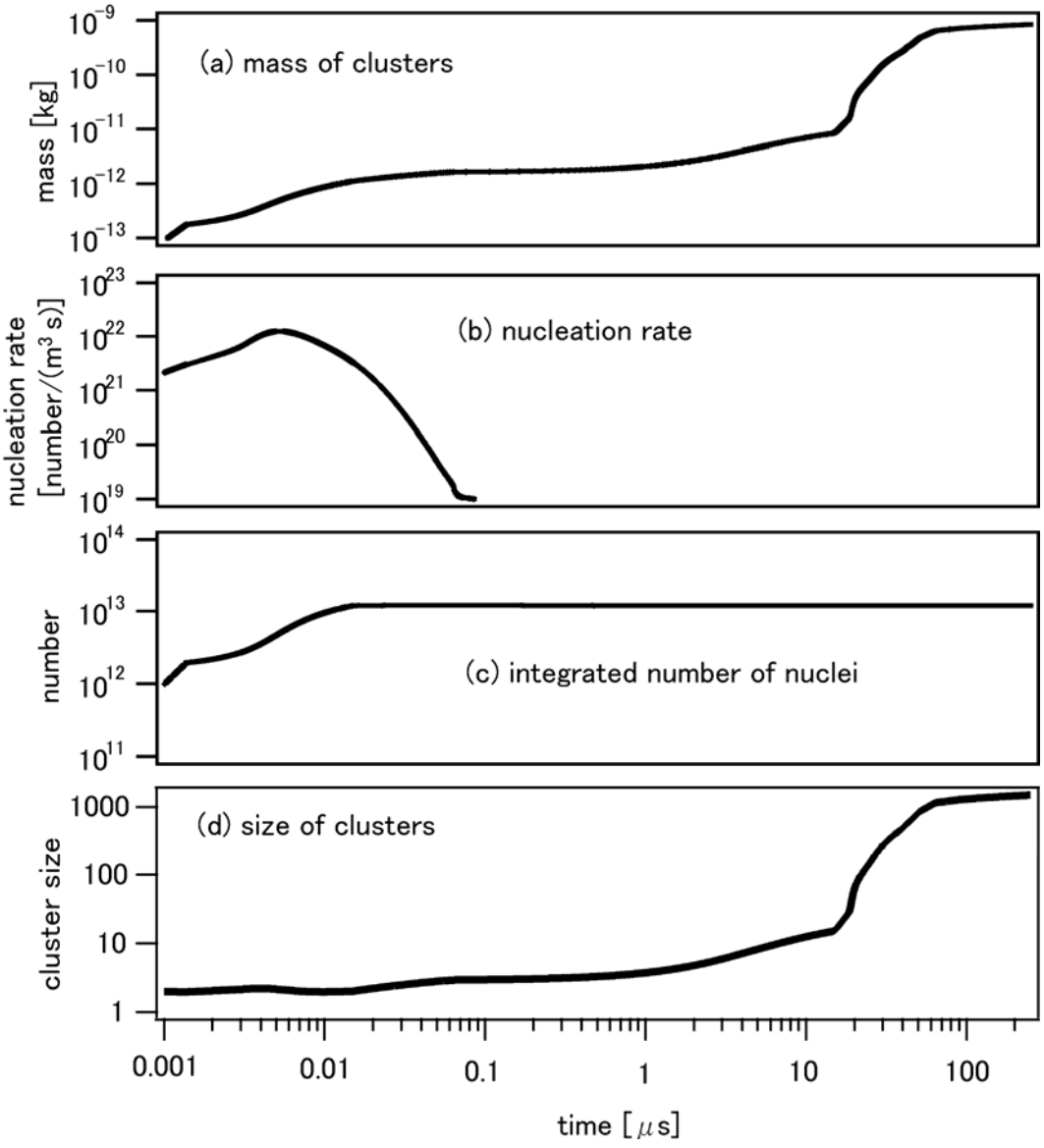

Fig.3. Variation of (a) the total mass of the generated Si nanoparticles in the enclosed space, (b) the averaged nucleation rate, (c) the total number of the nanoparticles and (d) the radius of the nanoparticles averaged based on the nanoparticle density distributed in the space.

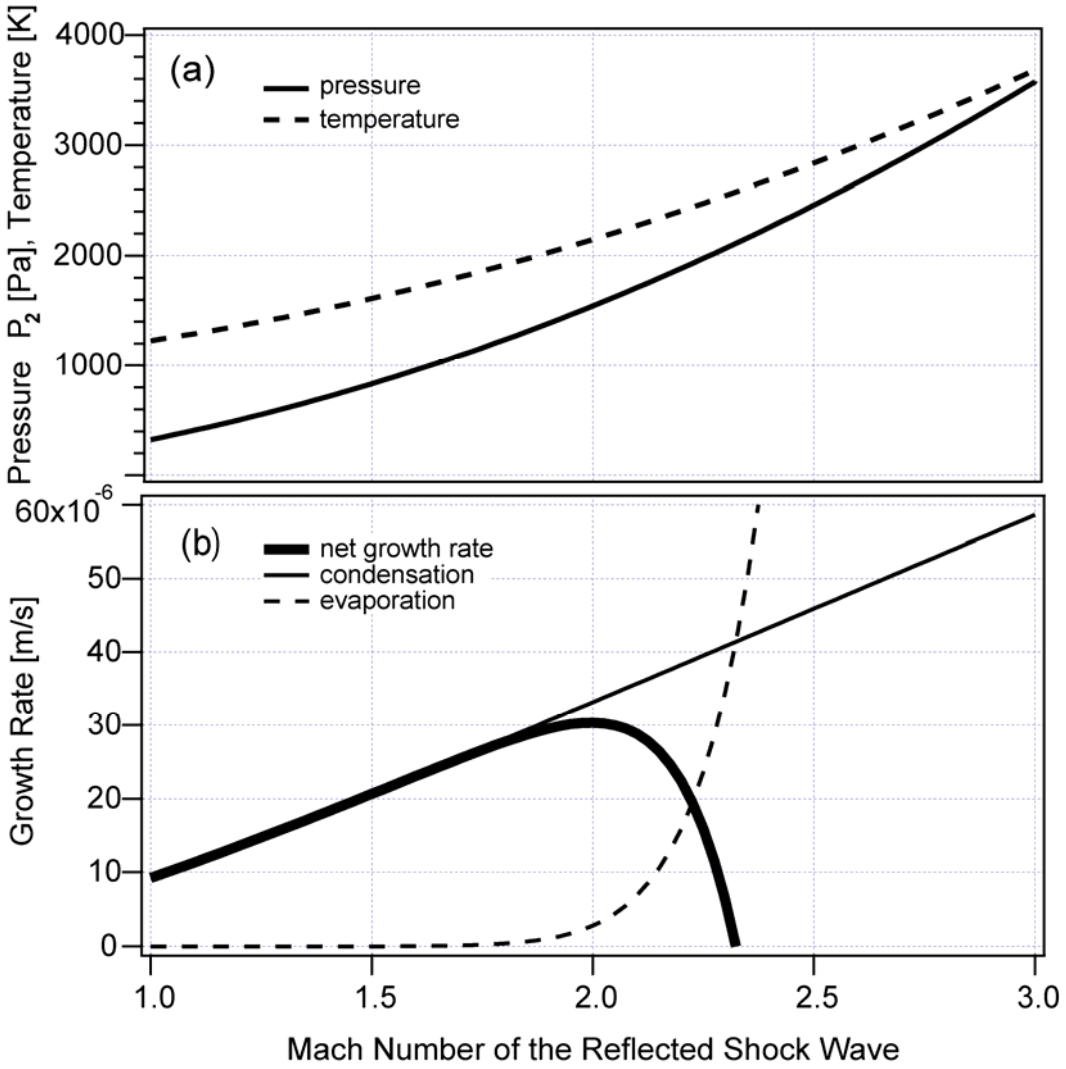

Fig.4. Changes after the reflected shock wave passed through the plume. (a) the pressure and temperature behind the shock wave, (b) the net growth rate of nanoparticle, condensation rate and evaporation rate.

Received: October, 2009